Plasma Sci. Technol. **26** (2024) 075507 (11pp) https://doi.org/10.1088/2058-6272/ad3615

Investigations on MoS_2 plasma by infra-red pulsed laser irradiation in high vacuum

Lorenzo TORRISI[1], Letteria SILIPIGNI[1], Alfio TORRISI[2] and Mariapompea CUTRONEO[1,3]

[1] Dipartimento di Scienze Matematiche e Informatiche, Scienze Fisiche e Scienze della Terra, MIFT, Università di Messina, Messina 98166, Italy
[2] Faculty of Medicine and Surgery, Kore University of Enna, Enna 94100, Italy
[3] Nuclear Physics Institute of the CAS, Husinec Řež, Prague 25068, Czech Republic

E-mail: lorenzo.torrisi@unime.it

Received 23 January 2024, revised 7 March 2024
Accepted for publication 20 March 2024
Published 27 June 2024

Abstract

MoS_2 targets were irradiated by infra-red (IR) pulsed laser in a high vacuum to determine hot plasma parameters, atomic, molecular and ion emission, and angular and charge state distributions. In this way, pulsed laser deposition (PLD) of thin films on graphene oxide substrates was also realized. An Nd:YAG laser, operating at the 1064 nm wavelength with a 5 ns pulse duration and up to a 1 J pulse energy, in a single pulse or at a 10 Hz repetition rate, was employed. Ablation yield was measured as a function of the laser fluence. Plasma was characterized using different analysis techniques, such as time-of-flight measurements, quadrupole mass spectrometry and fast CCD visible imaging. The so-produced films were characterized by composition, thickness, roughness, wetting ability, and morphology. When compared to the MoS_2 targets, they show a slight decrease of S with respect to Mo, due to higher ablation yield, low fusion temperature and high sublimation in vacuum. The pulsed IR laser deposited MoS_x (with $1 < x < 2$) films are uniform, with a thickness of about 130 nm, a roughness of about 50 nm and a higher wettability than the MoS_2 targets. Some potential applications of the pulsed IR laser-deposited MoS_x films are also presented and discussed.

Keywords: MoS_2, laser ablation, plasma, ion acceleration, quadrupole mass spectrometry, PLD

(Some figures may appear in colour only in the online journal)

1. Introduction

Molybdenum disulfide (MoS_2) is an inorganic compound belonging to the family of transition metal dichalcogenides. The MoS_2 bulk structure consists of stacked S-Mo-S sandwiches, which are held together by weak van der Waals interactions [1].

This compound has a molecular mass of 160 amu, a mass density of 5.06 g/cm^3 and a melting point of 2375 °C. It is stable in air, insoluble in water and diamagnetic. MoS_2 is widely used as a dry lubricant because of its low friction coefficient and robustness [2]. At room temperature, its thermal conductivity is about 6 W/mK [3] and it is a semiconductor material with a band gap energy of 1.23 eV [4] that increases to 1.8 eV in changing from bulk to single layer. Moreover, the nature of the band gap also changes from indirect to direct when switching from bulk to single layer (minimal sandwich).

MoS_2 possesses high mechanical strength with a measured value of the in-plane Young's modulus of a monolayer of 265±13 GPa [5]. It has a bulk electrical conductivity of about 10^{-4} Ω^{-1} cm^{-1} at room temperature [6]. When it is in the form of a monolayer or thin film, being a direct gap semiconductor, it can emit light, opening possible applications such as photodetectors. In fact, it is more and more employed in microelectronics to realize field-effect transistors (FET), biosensors, digital electronics, components of flexible electronic circuits or of photoelectrochemical cells [7], photoemitters and photodetectors [8, 9]. It is also used in chemistry as a catalyst for some important reactions [10] and

in the form of nanoparticles employed in different fields [11].

MoS_2 film deposition can be obtained using various physical and chemical approaches, such as chemical vapor deposition (CVD) [12], chemical exfoliation [13], spin-coating [14], electrodeposition [15], ion sputtering [16], pulsed laser deposition (PLD) [17], and others. As for PLD, sometimes it shows inconveniences for the sulphurated compounds deposition due to the low sublimation point of sulfur in high vacuum conditions. Moreover, MoS_2 thin films can be obtained by PLD in a vacuum using IR, visible and ultra-violet (UV) ns lasers [18–20]. Literature reported that stoichiometric films can be obtained using UV lasers promoting photo-chemical processes [21], while IR lasers promoting photo-thermal processes could be less suitable for depositing them. Therefore, the aim of the present investigation is threefold:

(1) to verify the possibility of using PLD with a pulsed IR (1064 nm wavelength) ns laser, instead of a UV one, for depositing thin films of MoS_2, highlighting its vantages and disadvantages;

(2) to evaluate the stoichiometry of the so-obtained thin films;

(3) to study the mechanisms of plasma generation in the condition of ns photo-thermal ablation.

Although the literature reported that stoichiometric and uniform MoS_2 films can be obtained using PLD with UV lasers [19], the use of pulsed IR lasers would have the advantage of being more reproducible and economical as these lasers are more versatile and stable than UV ones. The $I\lambda^2$ factor indicates that not only the laser intensity, I, but also the wavelength, λ, modifies the ablation yield, as reported in the literature [22]. This aspect is very important for the comparison between UV and IR lasers. In the case of UV lasers, due to their low intensity and wavelength, the ablation efficiency is low with respect to IR ones, and many pulses and irradiation time are needed to produce a thick deposition film. In fact, IR lasers have the advantage of being used to create films of large dimensions and greater thickness in less ablation time with respect to UV ones.

As laser power density (W/cm^2) and wavelength of the laser increase, the ablation yield (ablated molecules per laser shot), the ion energy, and the plasma temperature and density increase, producing a high flux of energetic atoms and molecules towards the substrate to be covered. The control of the intensity through the laser pulse energy, duration and focalization is crucial for the morphological aspect of the photo-deposited film because there is the risk that nanoparticles, debris and unwanted defects can occur in the morphology of the deposited film.

However, even if MoS_2 has been known since the eighties, there is poor knowledge about plasma composition, temperature, and ion energies obtained during PLD using IR ns laser pulses. Moreover, the film stoichiometry can undergo changes due to the different PLD setups, such as laser parameters, irradiation conditions and target and substrate nature.

In particular, it is important to do further investigations about the high plasma temperature in a high vacuum which could produce sulfur sublimation modifying the stoichiometry of the generated vapor and of the consequent deposited thin film [23].

In our experiments, the molybdenum disulfide film was deposited on a graphene oxide (GO) substrate for its properties that permit to realization of innovative micro- and macro-optoelectronic devices as optical filters, transistors and sensors, as reported in the literature [24–26].

The use of MoS_2 deposited on GO substrate is investigated to realize a new sensor type that may convert energy absorbed by GO (though X-ray absorption, ion energy loss, UV radiation) in characteristic luminescence from the thin MoS_2 film. Preliminary measurements demonstrate that, during the GO reduction, the electrical and optical properties of the system GO/MoS_2 are modified changing the MoS_2 visible luminescence induced by the UV lamp source.

The motivations and objective of this paper contribution consist in the presentation of PLD of thin MoS_2 films using the fundamental wavelength (1064 nm) of an Nd:YAG laser, one of the more stable and reproducible laser present in many laboratories in the world, which represents a simple, reproducible, well controllable and low-cost method to deposit complex thin films in vacuum on different substrates, as well as those that are very delicate and susceptible to compositional and structural changes based on graphene oxide.

Therefore, in this work, we used the PLD technique with ns IR laser pulses to produce MoS_2 films on GO [27] substrates for a better insight into possible applications in optoelectronics and nanotechnology.

To reach this purpose, the IR laser-generated plasma was characterized, and the pulsed IR laser-deposited film was analyzed to highlight the advantages and disadvantages of this technique.

2. Experimental set-up

An Nd:YAG pulsed laser (Litron TRLi850) was used at the 1064 nm fundamental wavelength, 5 ns pulse duration, maximum pulse energy of 1 J, in single pulse or at the 10 Hz repetition rate, to irradiate MoS_2 targets in high vacuum (~10^{-6} mbar). The Gaussian laser beam was focused by a 50 cm focal lens, and placed in air, on the target surface with a spot size of about 0.5 mm^2. Thus, the maximum laser intensity was $I \sim 4\times10^{10}$ W/cm^2 and the maximum laser fluence was $F \sim 180$ J/cm^2.

Four laser fluences were used: 40, 80, 120 and 180 J/cm^2. The incidence angle of the laser beam was maintained at about 0° during the laser ablation and the PLD of thin films.

The substrates that collect the photo-deposited film are placed parallel to the surface of the irradiated target and approximately 10 cm away. The temperature of the substrates was maintained at room temperature, although a minimum heating of the substrate to approximately 100 °C

was found by the plasma generated by 600 mJ pulse energy with a continuous deposition of 30 min at 10 Hz repetition rate.

For the measurements of ion velocity, the incidence angle was 45° in order to send the emitted ions toward an ion collector (IC), placed at a 1 m distance from the target (the flight distance), thus permitting the photon and ion detection as a function of the time from the laser shot by using the time-of-flight (TOF) technique.

A pure MoS_2 crystalline target with a thickness of about 0.5 mm and a surface of about 2 cm^2, bought from Sigma Aldrich, was employed to be irradiated in the single pulse mode or using a 10 Hz repetition rate during the PLD process.

PLD was employed to deposit thin films on graphene oxide substrates placed at about 10 cm distance from the target during laser irradiation at a 10 Hz repetition rate with a 600 mJ pulse energy.

The ablation yield, in terms of removed mass per laser pulse, was measured as a function of the laser fluence.

The produced non-equilibrium plasma was investigated with different instrumentations and techniques:

(1) IC detector connected to a fast storage oscilloscope (Tektronix TDS 5104B, 1 GHz, 5 GS/s) for the ion velocity TOF measurements.

(2) Quadrupole mass spectrometry (QMS, Pffeifer PrismaPlus HPA 220) equipped with a secondary electron multiplier and operating in the (1–300) amu mass range with a sub-ppm sensitivity.

(3) Fast visible CCD camera (PixeFly-PCO with optical equipment) with a 1 μs minimum exposition time triggered by the laser shot.

(4) Surface profiler (Tencor P 10) for the crater shape investigation with a vertical resolution of 10 nm and scan length, with selectable velocity, of some millimeters.

A scheme of the used experimental set-up is displayed in figure 1(a), while figure 1(b) shows a photo of the MoS_2 target, glued on a graphite substrate, before the laser irradiation. Pristine and irradiated targets together with the deposited thin films on graphene oxide substrates were submitted to different analyses, such as optical and electronic microscopies, surface roughness, crater shape and wetting ability measurements.

IR laser-deposited films were characterized in composition both using the energy-dispersion X-ray (EDX) analysis and the Rutherford backscattering (RBS) spectrometry. In EDX analysis, 20 keV electron beams allowed us to monitor the fluorescence K- and L-lines of S and Mo respectively, while in RBS spectrometry, 2.0 MeV α-particles, accelerated by the 3 MV Tandetron of Canam (NPI, ASCR, Czech Republic), bombarded the investigated sample and then the backscattered α-particles were detected at a backscattering angle of 170° [28].

The laser-deposited film thickness, roughness and wetting ability were also measured using the Tencor-P 10 surface profiler and the sessile drop method. In this last analysis, a 1 μL distilled water drop was deposited on the laser-deposited film surface [29].

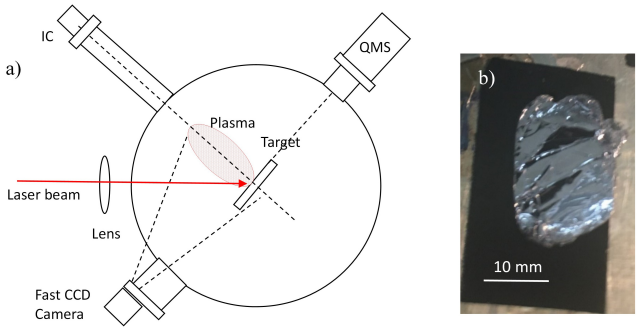

Figure 1. Scheme of the experimental set-up (a) and a photo of the MoS_2 target glued on the graphite substrate (b).

3. Results

The laser shots hitting the MoS_2 target placed in a vacuum produce ablation with the emission of highly ionized vapor, i.e., a plasma, which expands at high velocity in a vacuum decreasing exponentially its density as the time from the laser shot and the distance from the target increases. The ablation yield, evaluated in terms of removed mass per laser pulse, was measured by changing the laser fluence thanks to the crater volume evaluation through the surface profiler.

Figure 2 shows two crater depth profiles obtained using two different laser fluences: 80 J/cm^2 (a) and 120 J/cm^2 (b).

By evaluating the crater volume and the removed mass, applying a MoS_2 density at about 5.06 g/cm^3, the ablation yield grows with the laser fluence, as shown in figure 3. The error of measurements was evaluated at about 10%.

The relation between the ablation yield and the laser pulse fluence is about linear and slight non-linearity is expected, according to processes occurring in PLD from IR lasers. In fact, the minimum non-linearity effects are due to the ablation threshold of PLD by IR laser, expected to have low fluence because of the insufficient energy to produce evaporation, and to a saturation trend, occurring at high fluence because dense plasma partially absorbs the laser pulse, as reported in the literature [30].

The reported ablation yield data depend on many parameters such as the laser intensity, the $I\lambda^2$ plasma factor (being I the laser intensity and λ the wavelength), the irradiation conditions (incidence angle, focal distance from the target surface), and target geometry and composition [31]. In particular, the $I\lambda^2$ factor indicates that not only the laser intensity but also the wavelength modifies the ablation yield. Thus, in the case of UV lasers, due to their low intensity and wavelength, the ablation efficiency is low with respect to IR lasers, and many pulses and irradiation time are needed to produce a thick deposition film.

However, the ablation yield may also depend on other factors depending both on the parameters of the laser used (energy, pulse duration, polarization, ...) and on the irradiation conditions (spot size, vacuum, air, gas or liquids, ...) and the type of target (density, allotropic state, crystal orienta-

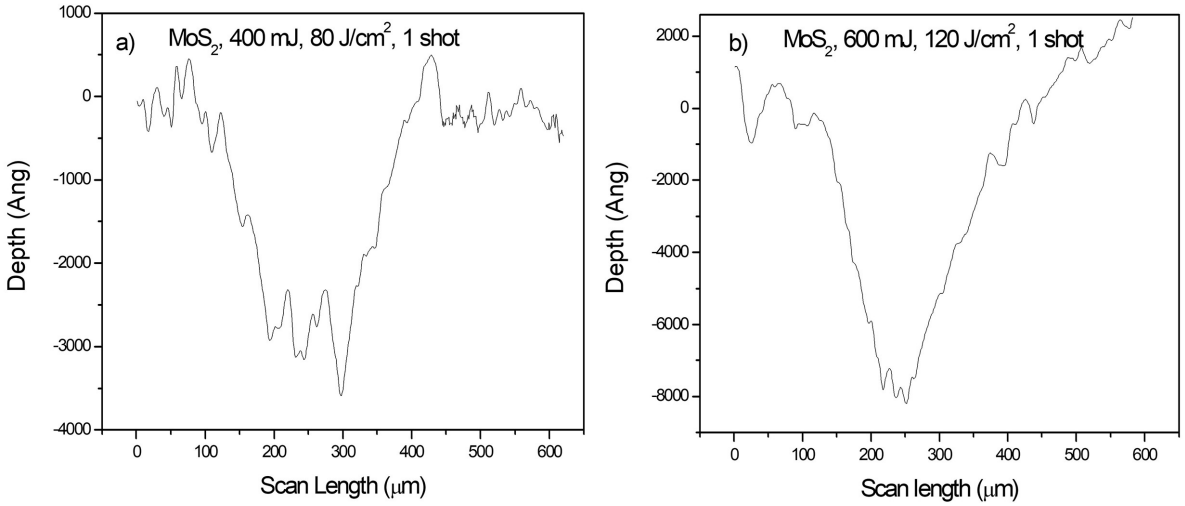

Figure 2. Crater depth profiles for laser irradiations at the fluences of 80 J/cm^2 (a) and 120 J/cm^2 (b).

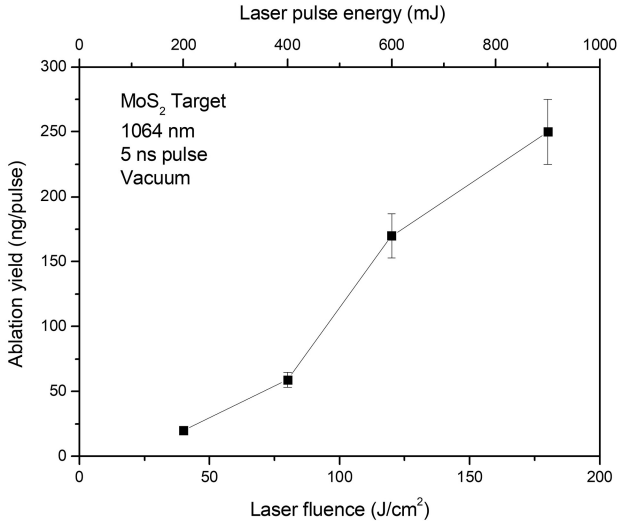

Figure 3. MoS_2 ablation yield versus 1064 nm laser fluence.

tion, temperature, ...). It may also depend on self-focusing effects in the preplasma produced in front of the target by the same laser pulse, as well as on vacuum sublimation effects that produce layers of gas in front of the irradiated target [32].

The IC measurements in the TOF regime, triggered by the laser shot, have permitted us to obtain a lot of information on the emitted ions and the properties of the produced plasma. Figure 4 displays some IC-TOF spectra relative to different laser pulse energies hitting the target in a single shot, from 200 mJ up to 800 mJ.

The spectra show a photopeak that forms at the instant of irradiation of the laser pulse and which indicates the zero of the time-of-flight scale. It is due to the photoelectric effect on the IC copper walls induced by the plasma photons emitted at the laser shot. Photopeak is followed by a large and intense ion peak which represents the convolution of different detected ions at different masses and charge states. The fastest ions are protons due to the hydrogen presence in each material.

Carbon and oxygen as contaminants and sulfur and molybdenum ions as compositional elements are also detected. On the base of the flight distance (1.0 m) and of the TOF measurement, spectra report the proton, sulfur and molybdenum ions' maximum energy measured along the normal direction to the target surface. The arrows in figure 4 are indicative of the ion energy in the indicated TOF values, evaluating the maximum proton energy (arrow at the minimum TOF peak value), maximum sulfur ion energy (at the peak ion distribution, being the sulfur the main plasma component with the lower atomic weight) and at about the maximum molybdenum ion energy (the second component of the plasma, less distinguishable due to its overlap at the tail of the TOF spectrum of sulfur ions).

Ions are accelerated by the produced non-equilibrium plasma, which, in terms of charge emission, emits the first fast (hot) and cold electrons and then slower ions, with a speed inversely proportional to their mass. Thus, the first protons are detected, followed by the S ions and Mo ions, of which the fastest are the most ionized species.

Assuming the ion acceleration to be dependent on the proton acceleration per charge state due to the electric field developed in the plasma, the IC-TOF spectra indicate that S could be ionized up to 14^+ and Mo up to 19^+. Thus, their maximum energy is approximately given by the maximum charge state by the proton energy, according to the references [33, 34]. For example, at the 200 mJ laser pulse energy, the maximum proton energy is about 20 eV, while the maximum energies of the S and Mo ions are about 266 eV and 340 eV, respectively. Thus, the maximum charge states of S and Mo ions correspond to $266/20 \approx 13^+$ and $340/20 \approx 17^+$, respectively. Carbon and oxygen ions are also present, with a maximum energy between that of protons and sulfur ions, but as contaminants, their small contribution can be neglected.

The photopeak intensity and the maximum energy of protons, sulfur and molybdenum ions change with the laser pulse energy, as shown in the plots of figure 5. In fact, the photopeak intensity decreases with the laser pulse energy. On the base of the literature, its yield could contain also luminescence induced by both the laser pulse on the target

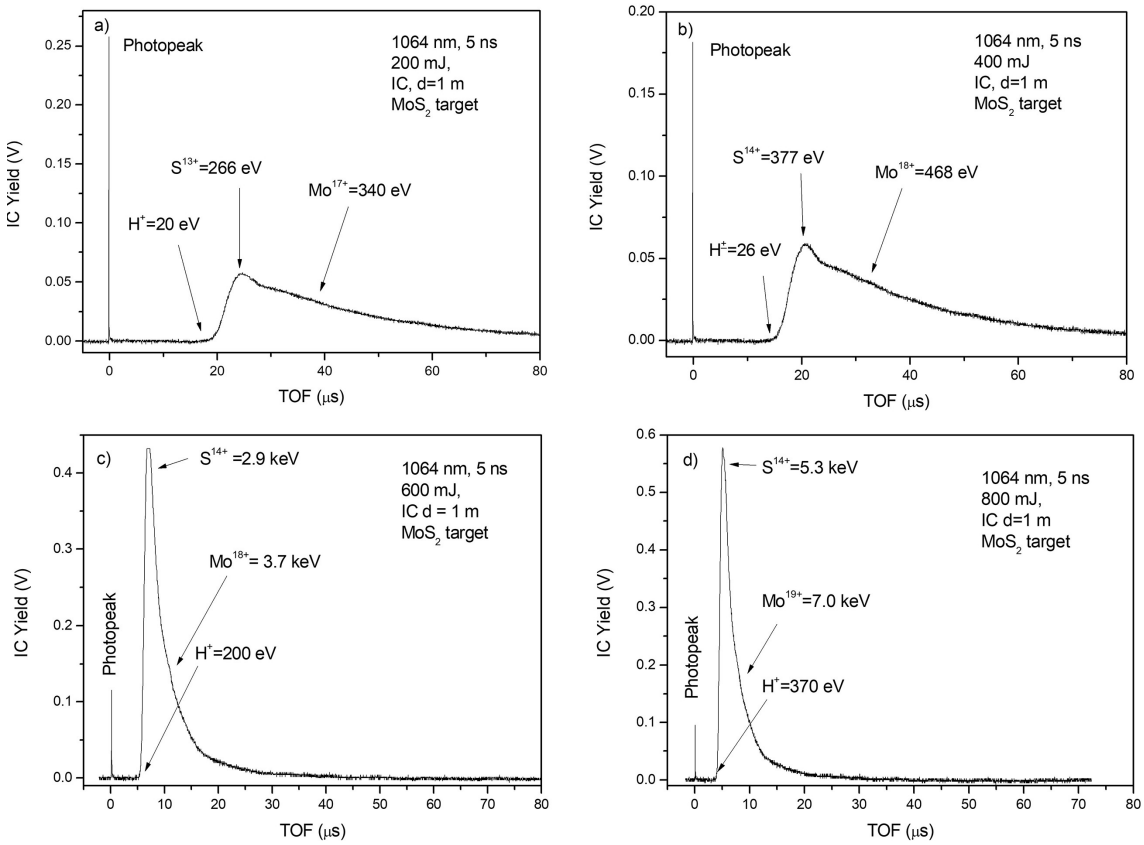

Figure 4. IC-TOF spectra relative to the MoS_2 target irradiation at 200 mJ (a), 400 mJ (b), 600 mJ (c) and 800 mJ (d).

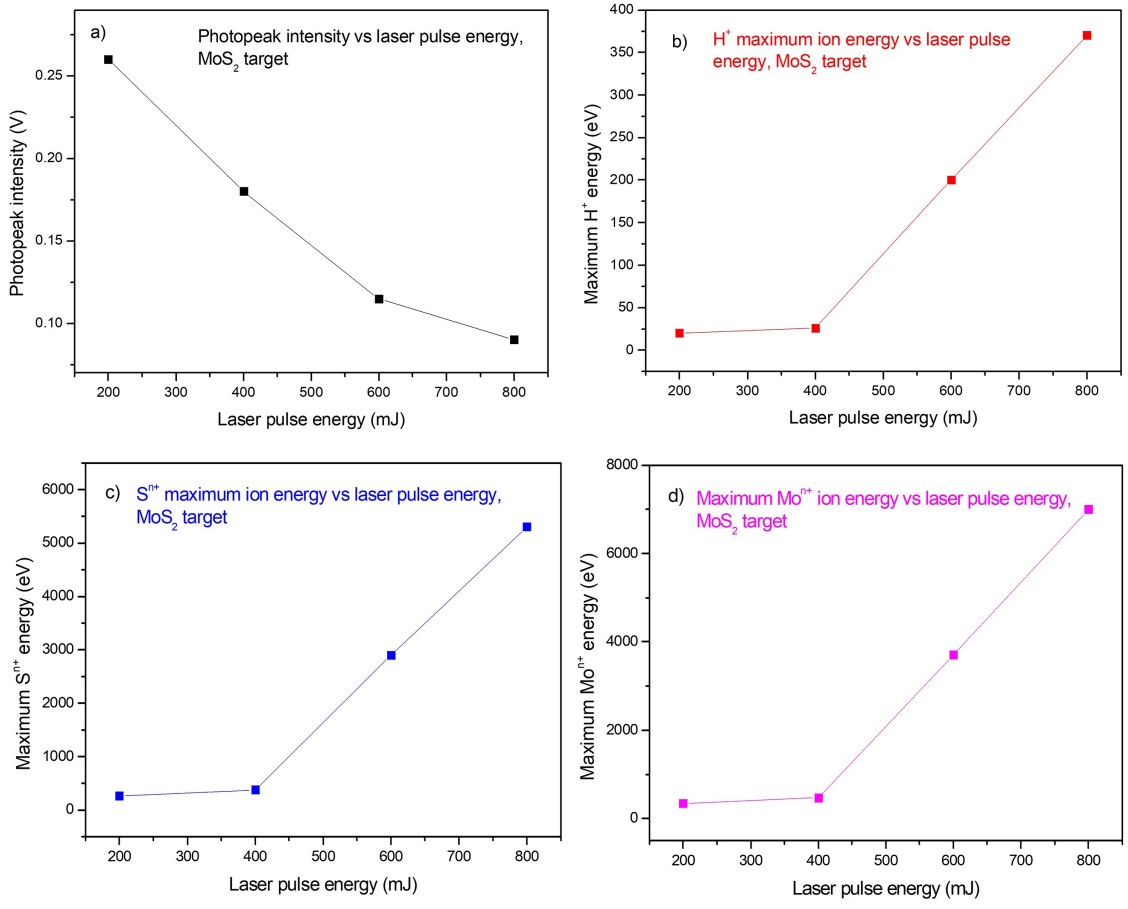

Figure 5. Photopeak intensity (a) and maximum energy of H^+ (b), S^{n+} (c) and Mo^{n+} (d) versus laser pulse energy.

and the S and Mo deexcitation photons [35]. In this case, luminescence could be more intense using low laser pulse energy and decreases at high laser pulse energy at which a hot and dense plasma is generated and luminescence could be partially absorbed by it.

On the contrary, the ion energy grows with the laser pulse energy, as expected, due to the highest electric field driving their acceleration, which is proportional to the plasma electron density and temperature, as reported in the literature [36]. The measured maximum ion energy for S and Mo, up to about 5 keV and 7 keV at the 800 mJ laser pulse energy, indicates that the deposited film is composed of the evaporated and low energy atoms removed from the target and by energetic ions accelerated by the developed plasma. These last can be implanted in the first superficial layers of the substrate conferring high thin film adhesion. The use of successive laser pulses, incident on the same position on the target, shows an important effect of sulfur ion yield decreasing, as illustrated in figure 6 for laser pulse energy of 400 mJ hitting MoS_2. This result can be due to a different ablation yield for the Mo and S atoms and to the reduction for S because it is partially sublimated by the high target temperature. In fact, sulfur at room temperature sublimates in a vacuum due to its low fusion temperature of only 115 °C at 1 atm pressure and lower at lower pressure [37, 38]. Sulfur vapor is produced in the vacuum chamber, as will be discussed in the following part, and removed through the high speed of the used turbomolecular pump. Thus, the MoS_2 target heating by repetitive laser ablation may decrease the contribution of the sulfur in the fused material, especially if partially dissociated from Mo in the zones around the ablated crater.

The figure shows that the photopeak intensity and the ion energy remain unchanged with the repetitive laser shots but that the sulfur ion peak yield significantly decreases with the repetitive laser shot as is evident in the third shot (b) and in the sixth shot (c) with respect to the first shot performed on fresh surface (a). It is also evident that the ablation yield decreases. In fact, the maximum IC yield of 0.06 V, obtained at the first shot, decreases to 0.034 V at the third shot and to 0.026 V at the sixth shot. This result can be due to the laser beam becoming defocused, which occurred during the crater ablation, or due to a decrement of the sulfur component in the irradiated target surface.

Some important characteristics of the obtained plasma can be derived from the acquired measurements in a vacuum. For example, in a first approximation, the plasma temperature and the ion plasma density can be evaluated. We plan to characterize the plasma obtained using a 400 mJ laser pulse, under the conditions used for the deposition of the MoS_2 film in vacuum. In such conditions, the maximum evaluated ionization of S and Mo is 14^+ and 18^+, respectively (see figure 6(a)). It is possible to know the ionization potentials involved in the ionization process using the NIST database [39]. The ionization potentials of S^{13+} and Mo^{17+} are 707 eV and 702 eV, respectively. The ionization potentials of S^{14+} and Mo^{18+} are 3224 eV and 758 eV, respectively.

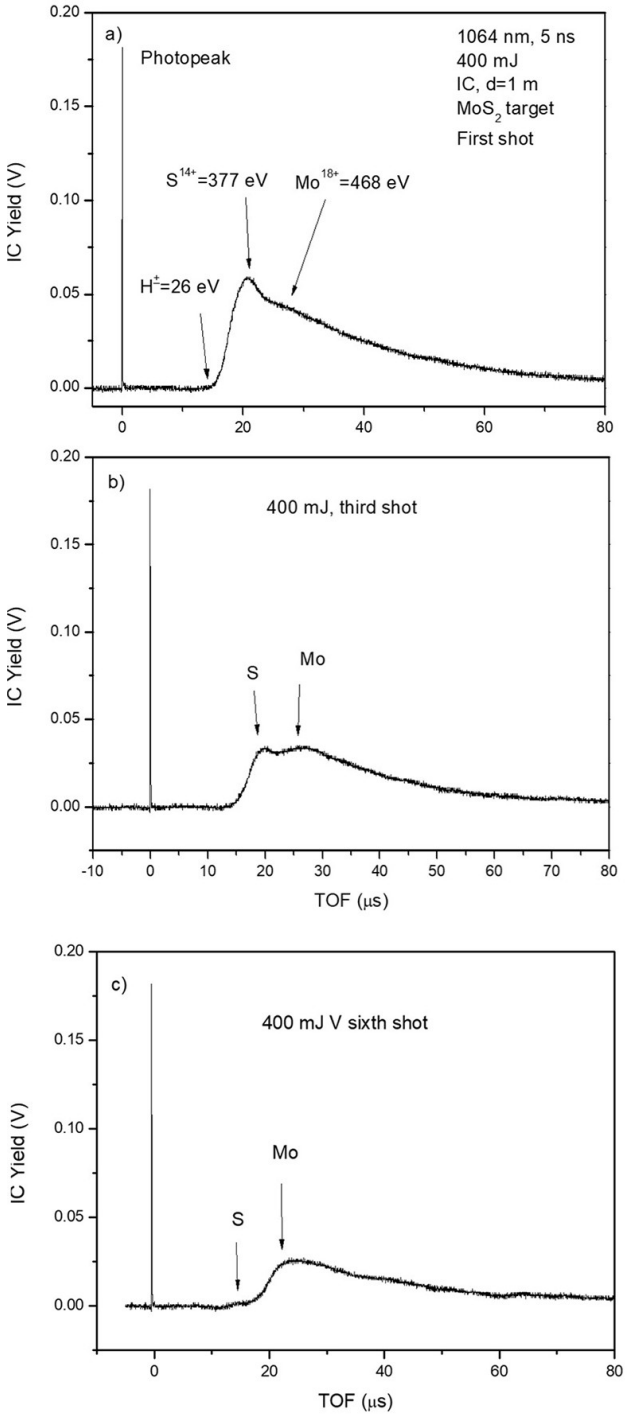

Figure 6. IC-TOF spectra for the MoS_2 target irradiated at the first shot on fresh surface (a), at the third shot (b) and the sixth shot (c) on the same laser spot position.

This means that electron energy has a maximum value of about 710 eV, permitting the ionization of S^{14+} and Mo^{18+} but not of the higher charge states. Assuming this maximum electron energy to be of about 710 eV, and their energy distribution to be a Boltzmann type, the medium electron energy $<E>$ is about a fifth of the maximum one, i.e. $<E> \sim 142$ eV, thus the mean plasma temperature $<kT>$ is:

$$< kT >= 2E/3 \sim 95 \text{ eV}. \quad (1)$$

The laser-generated plasma at the 400 mJ pulse energy was photographed in visible light using a fast CCD camera with a 1 μs exposition time triggered by the laser shot, as shown in figure 7. The hot plasma has a white color (higher light intensity and plasma temperature) while the cold plasma decreases in temperature with the gray colors up to the black one. From this image, an approximated evaluation of the plasma volume has been obtained. Assuming its ellipsoidal shape with a length of 0.8 cm and a width of 0.6 cm, its volume at 1 μs from the laser shot is approximately V = 0.15 cm^3.

The mass removed per pulse at the fluence of 80 J/cm^2 was about 59 ng, corresponding to about N_m = 2.2×10^{14} molecules/pulse. Assuming all the removed mass to be ionized and assuming the visible image to be due to the ion deexcitation emitted during the ablation, the ion plasma density, n_i, can be evaluated about:

$$n_i = \frac{3\times N_m}{V} = \frac{3\times 2.2\times 10^{14}\ \text{ions}}{0.15\ \text{cm}^3} = 4.40\times 10^{15}\ \text{ions/cm}^3. \quad (2)$$

Of course, this value is higher during the laser shot and quickly decreases with time and the distance from the target surface, as reported in the literature [40].

The electron density is higher with respect to the ion one and it depends on the mean charge state distribution of the ions, which should be evaluated as a function of the time [41]. However, due to the highest probability of ionization of the low charge states 1+, 2+ and 3+ at which the ion recombination probability is lower, in a first approximation, it is possible to assume that the mean charge states are within about 2+ and 3+, thus the plasma electron density is about double or triple with respect to the ion one reported in equation (2) [42].

The MoS_2 laser ablation process was also monitored by the QMS spectrometer. It was used to detect the residual gas in the vacuum chamber and not detect the directly emitted ions from the laser ablation. In fact, its position does not allow to detect the direct ions emitted from the irradiated target. It was used to fix the masses of interest and follow their evolution with time starting from the laser shot in single and multiple laser pulses. The following masses by QMS spectrometry were: H_2 (2), H_2O (18), S (32), H_2S (34), SO (48), S_2 (64), Mo (96), MoH_2 (98), MoO (112), MoS (128), and MoS_2 (160).

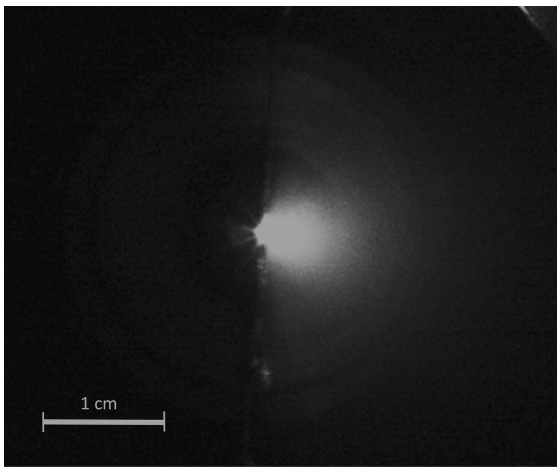

Figure 7. Visible CCD plasma image acquired in a time of 1 μs triggered with the laser shot (400 mJ).

Some QMS spectra are displayed in figure 8 for the selected elements versus time indicating the laser-on and laser-off switch times. The background is measured during the laser switch-off and the useful signals of the gases present in the vacuum chamber, during the laser switch-on, are detected.

Figure 8(a) shows the QMS spectra of the main elements for two single laser shots, indicating that the amount of atomic and molecular ablation emission decreases exponentially, from the H_2O to S, Mo, MoO, SO, S_2, MoS and MoS_2.

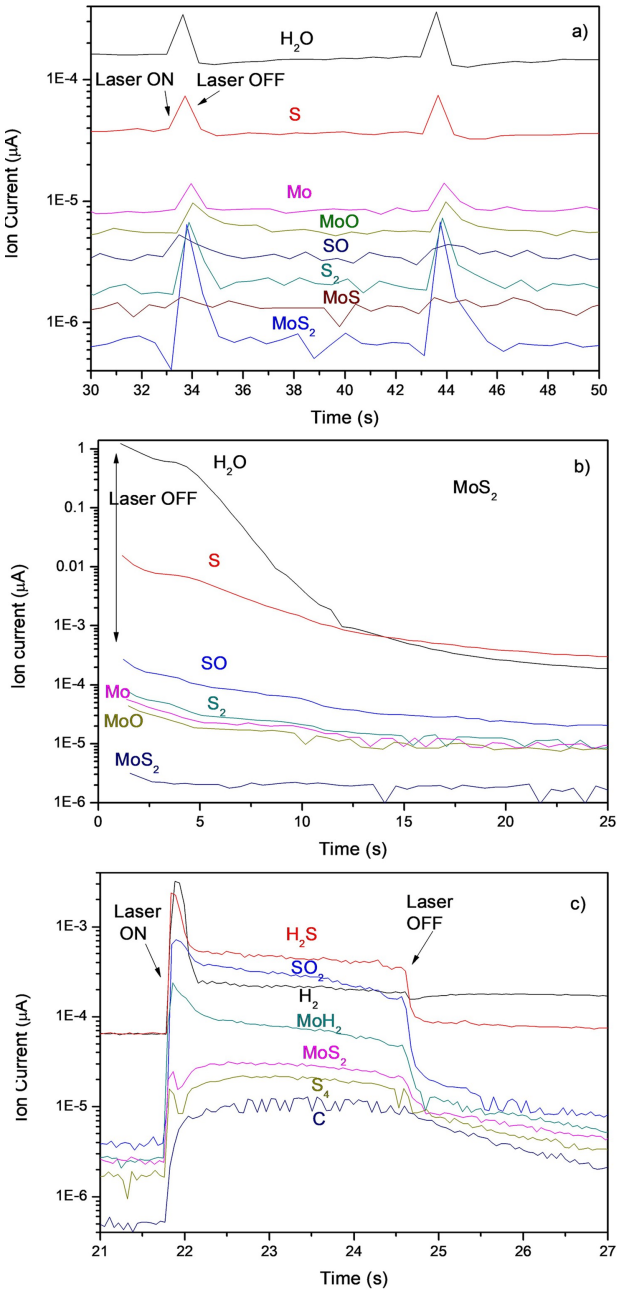

Figure 8. QMS spectra of main elements in single laser pulse (a), in the transient at the laser switch-off after a repetition rate prolonged irradiation (b) and of some investigated compounds (c).

Thus, the most evident emission is that of S atoms followed by that of Mo ones, and the less evident one is that of MoS_2 molecules. No MoS emission occurs. The S/Mo emission yield ratio is about 5.3, indicating that the atomic emission is not stoichiometric because a stronger emission of sulfur with respect to Mo occurs. This ratio, in fact, is more than double with respect to the stoichiometric value of 2.0.

It is possible that some S is reacting with the residual gas (water vapor) to remain gaseous and it does not react with Mo but it is also possible that S is being removed from the vacuum chamber via the turbo-molecular pump. We have not been able to carry out measurements at various pressures because for the correct functioning of the quadrupole mass spectrometer a high vacuum of not less than 10^{-5} mbar must be used, otherwise, the filament of the detection instrument would skip.

Figure 8(b) displays the QMS spectra in the transient at the laser switch-off after a long duration of repetition rate irradiation of the target (15 min) at which a stable atomic and molecular emission was obtained (during the pulse laser deposition of the thin film). The transient shows an exponential decay of the emitted main species, which in order decrease from H_2O to S, SO, S_2, Mo, MoO and MoS_2. It confirms that the maximum emission is that of S, followed by that of Mo; that of the MoS_2 molecular emission, as gas, is practically negligible, because about three orders of magnitude lower than that of S and very near to the background signal. In this case, it is measured a S/Mo yield ratio of about 100, probably due to the accumulation of S vapors during a long time of laser ablation.

We want to remind here that QMS does not report the direct emission of the target which gives rise to the deposited film, but it informs us about the various types of gaseous species formed in the chamber during the long laser ablation. The deposited film, on the other hand, has grown in front of the target and receives the ionic and neutral species, of low and high energy, emitted by the hot plasma, so it could be perfectly stoichiometric or at most with a slight reduction of sulfur compared to the original stoichiometry of the target.

Figure 8(c) shows some QMS spectra relative to molecular compounds produced during the repetitive laser ablation in a vacuum, due to the laser beam inducing ionizations, molecular dissociations, and radical formation. Such effects can produce chemical reactions in the plasma, generating some compounds such as H_2S, SO_2, H_2, MoH_2, MoS_2 and S_4. The higher contribution is that of some hydrogenated molecules, such as H_2S, H_2, and MoH_2. Also, SO_2 shows significant levels of production. For example, S could react with H_2O (vapor) through the reaction:

$$3S + 2H_2O\,(\text{vapor}) \rightarrow 2H_2S + SO_2 \qquad (3)$$

The emissions of MoS_2, S_2 and S_4 molecules are less evident. For comparison also carbon ablation, as a contaminant, is reported. Results indicated that hydrogen is present in the irradiated target, O and C also as contaminants. However, H, O and C can be emitted not only from the target as absorbed gases but also from the vacuum chamber walls which desorb under the use of a laser beam at the repetition rate of 10 Hz for long times (10–30 min).

The PLD of MoS_2 thin films on GO was performed using a 400 mJ laser pulse energy, a 10 Hz repetition rate and an irradiation time of 30 min. Figure 9 shows two photos in optical microscopy of the deposited thin film on the GO substrate. Figure 9(a) highlights the uniformity of the deposited thin film, while figure 9(b) is relative to the MoS_2 thin film/GO substrate interface. A mask to cover the substrate borders was used during the MoS_2 thin film deposition.

The film is formed by a distribution of single micro- and sub-micrometric crystals, which generate a uniform monolayer thickness. The white spots observed in optical microscopy are due to the peculiar properties of the MoS_2 thin film, which shows the effects of visible reflectance and luminescence of their crystalline nucleated dots, according to the references [43, 44]. A part of MoS_2 micro and nanostructures diffuse under the mask used to cover the GO substrate, which is not perfectly planar, and is also visible as bright spots.

Measurements of the thin film surface profile have permitted to evaluate the film thickness and roughness, taking into account the surface of the underlying GO substrate which is not perfectly planar, and which shows flaking effects, typical of this material, and the very reduced thickness of the photo-deposited films.

Figure 10 shows a spectrum of profilometry at the GO-

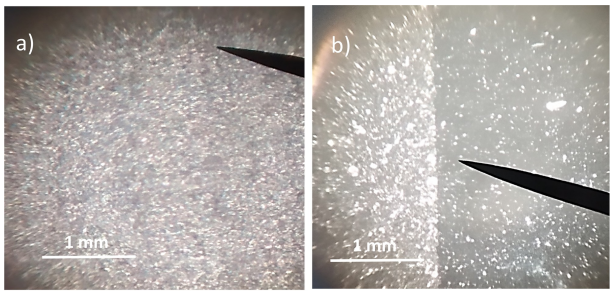

Figure 9. Optical microscopy of the MoS_2 film deposited on the GO substrate (a) and the interface between the film and the substrate (b).

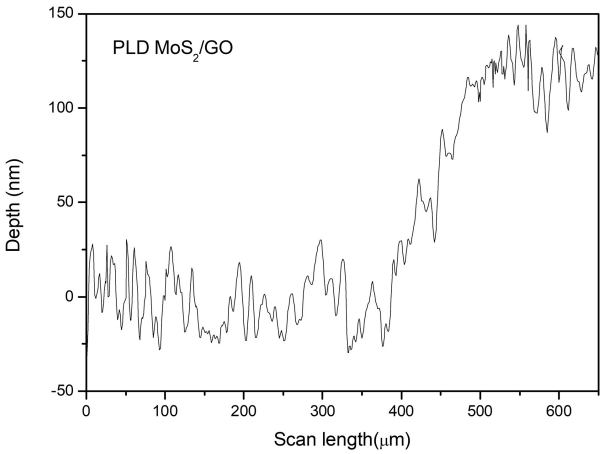

Figure 10. Profilometry of the GO (substrate)-MoS_2 PLD film interface.

MoS_2 deposited film interface. The film thickness is about 130 nm and the roughness, referred to as its average value, is of the order of 50 nm. The film thickness agrees with the ablation yield at the 400 mJ and 80 J/cm^2 fluences and for substrates placed at about 10 cm distance from the target, orthogonally to its surface considering a particle emission along the normal to the target surface within a solid angle of about π steradians.

Two important parameters to be controlled are the laser repetition rate frequency and the total irradiation time, which change the thin film deposition velocity and thickness. Of course, increasing the laser irradiation time above 30 min it will be possible to enhance the deposited film thickness. The MoS_2 thin film uniformity, instead, depends a lot on the surface conditions of the substrate which, if not perfectly planar, have repercussions on the morphology of the thin films deposited on it. In the case of GO, for example, the initial surface is certainly not as planar as in glass and silicon substrates and therefore the found roughness of the deposited films can largely be attributed to such irregularities and surface flaking of the substrate. Literature [45], in fact, reported numerous articles regarding the replication of the roughness of the substrate on the growth of the deposited thin film.

The target and the film stoichiometry have been determined using both EDX and RBS analyses, which are in good agreement. Figures 11(a) and (b) display the SEM image of the target surface and its EDX spectrum, respectively. While figures 11(c) and (d) show the SEM image of the uniform deposited thin film and its EDX spectrum, respectively. The quantitative analysis performed with reference standards, using a 20 keV electron beam, demonstrated that the target stoichiometry is MoS_2, being the S/Mo atomic ratio equal to 2.0. Instead, the stoichiometry in the PLD thin film is deficient in sulfur giving an atomic ratio S/Mo equal to 1:1.

The stoichiometry of the PLD film was also controlled using the 2.0 MeV RBS spectrometry (see table 1). It evinced that the deposited film contains less sulfur with respect to the pristine target. In fact, the S/Mo atomic ratio decreases from 2.0 to about 1.3. This result agrees with the EDX measurements and IC-TOF spectra. Indirectly, also the QMS measurements indicate that the PLD film should contain less sulfur due to its strong degassing observed during the laser ablation process in vacuum. The S decrement in the PLD film was evaluated in the order of 45% and 35% for EDX and RBS, respectively.

Thus, although high S vapor concentration occurs, the deposited film in front of the target remains about stoichiometric showing a decrement of sulfur concentration with respect to the pristine target. The obtained results agree with the literature data which report that sulfur deficiency, in terms of S vacancy defects, may occur during the MoS_2 growth in vacuum by PLD [19, 46, 47].

Measurements of wetting ability were conducted by

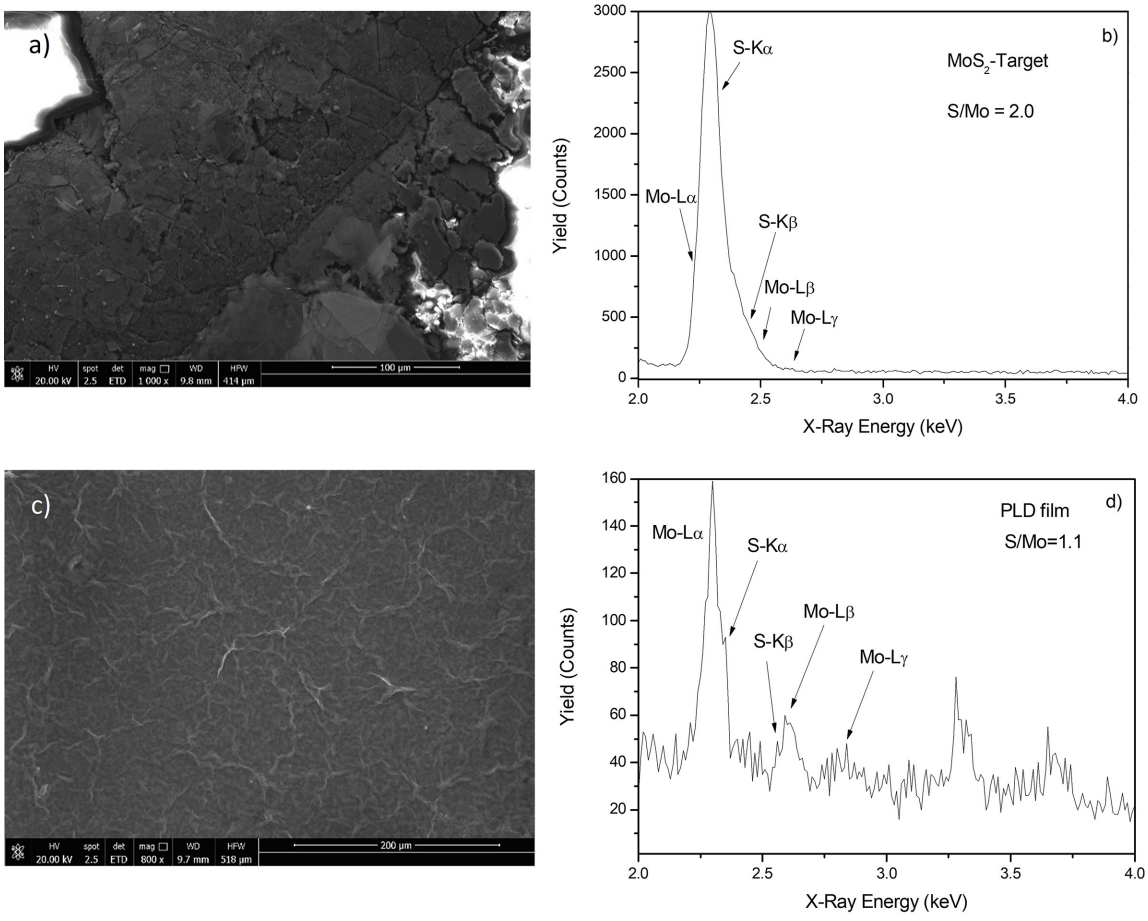

Figure 11. SEM images of the target (a) and of the PLD film (c), and EDX spectra of the target (b) and of the PLD film (d).

Table 1. EDX and RBS data comparison for the thick MoS_2 target and thin PLD film.

Analysis	S/Mo atomic ratio	
	Target	PLD film
EDX	2.0	1.1
RBS	2.0	1.3
References [19, 46, 47]	2.0	1.3–1.5

depositing 1 μL of distilled water on the pristine GO substrate surface, on the partially reduced GO substrate surface during PLD in vacuum due to the increase of plasma temperature, on the MoS_x thin film, about 130 nm thick and laser deposited on GO, and on the surface of the pristine and thick MoS_2 crystal target. A comparison of the results is shown in figure 12.

It indicated that the highest wetting ability is in the pristine GO which has a contact angle of about 60° (a), while in rGO, reduced by the plasma temperature during PLD in vacuum (GO under a thin mask to not be covered by MoS_2), the contact angle increases to about 73° (b). In the thin film laser deposited on rGO the contact angle is about 71°, while in the pristine MoS_2 crystal surface, the contact angle assumes the maximum value of about 92°, showing a clear hydrophobic surface, in accordance with the reference [48].

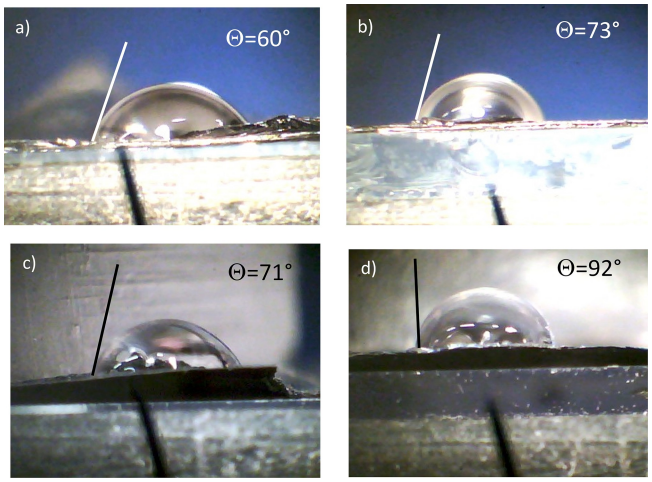

Figure 12. Contact angle measurements in the GO substrate (a), in the GO substrate after the PLD deposition (b), in MoS_x laser deposited film (c) and in the pristine MoS_2 target (d).

Further analyses are in progress to characterize the MoS_x film laser deposited on Si and quartz substrates using optical spectroscopies, Raman and FTIR spectroscopies. A better characterization will be performed also using electrical measurements, electron microscopy and X-ray diffraction analysis, as will be reported in the next paper.

Although not perfectly stoichiometric and not characterized from the point of view of the electrical properties, the obtained PLD MoS_x films can be employed for different applications, such as lubricant surfaces reducing wear due to their low friction coefficients, as optical filters for near UV region, as films with high mechanical resistance to shear strength, as films for microelectronics based on FET, and as photodetectors [18, 49, 50].

4. Conclusions

PLD of MoS_2 targets in high vacuum using a laser at a 1064 nm wavelength and with a 5 ns pulse duration was investigated. Measuring the crater volume of single laser shots was possible to evaluate the ablation yield (removed mass per laser pulse) as a function of the laser fluence.

From the IC-TOF measurements, the S and Mo ions' maximum energy and maximum charge state were evaluated. Using laser fluence within the range of 40–180 J/cm^2, the laser-produced plasma was characterized by giving the ion maximum energy and the photopeak emission versus the laser pulse, the mean temperature, the ion and electron density, and its expanding volume at 1 μs exposition time from the laser shot. IC-TOF measurements have demonstrated that the repetitive laser shot produces less emission of sulfur with respect to the first shot, indicating a possible sulfur decrement in the target composition.

Emitted atoms and molecules were analyzed using quadrupole mass spectrometry. Results have indicated that the maximum mass emission is due to the atomic emission of S and Mo, as expected. However, the S/Mo QMS yield is higher than 2, demonstrating that the S ablation is not stoichiometric with the Mo ablation. Moreover, the emission is accomplished by emissions of trace elements containing hydrogen, oxygen and carbon and of different compounds, such as Mo and S oxides.

Optical and electronic microscopies have indicated that the obtained PLD films seem to be uniform, with a thickness of about 130 nm and a roughness of about 50 nm. The composition of the MoS_x laser deposited films, measured using the EDX and RBS analyses, evinces an S decrement of the order of 35%–45% with respect to the pristine target, which is in good agreement with the literature data that reports S vacancy defects in MoS_2 films grown by UV PLD in vacuum.

Our investigation has highlighted some advantages of ns IR PLD technique such as the high energy of emitted ions, of the order of keV, generating ion implantation of Mo and S, which in turn induces high adhesion of the film to the substrate surface. Further benefits are the ease and speed of the PLD processing, its control of the film's thickness and high reproducibility. One of the main disadvantages of the PLD thin film, using our parameters, concerns its not-stoichiometry, leading to the deposition of a thin film of chemical formula MoS_x (with $1 < x < 2$).

Although the obtained films have a lower S content of about 35%–40% less and the stoichiometry is not exactly that of MoS_2 but rather that of MoS_x ($1 < x < 2$), the obtained films still have interesting applications to be used in different fields. The least amount of S, for example, increases the electrical conductivity of the compound, the films are soft and oily and, due to the weak van der Waals interactions, the film, even if depleted of sulfur, has a low coefficient of fric-

tion and can also be used as a solid lubricant. The films can be used as optical filters for the near UV region as the lower sulfur content increases the transmittance compared to MoS_2 films as preliminary measurements have demonstrated. The mechanical resistance remains almost unchanged compared to that of stoichiometric films, especially that of shear stress.

Microelectronics may use MoS_2 and MoS films due to their applicability to the drain-source current control from the gate polarization voltage in FET devices. Particularly our interest in the system GO/MoS_2 comes from the possibility of realizing luminescent micro devices under UV excitation.

Further analyses on the MoS_x IR laser deposited films are in progress to better characterize them from the point of view of morphology, composition, absorption, trace elements, crystallinity, and others. Electrical measurements will be also performed to evaluate the properties of the so-obtained PLD films.

Acknowledgments

The research has been realized at the CANAM (Center of Accelerators and Nuclear Analytical Methods) infrastructure LM 2015056. This publication was supported by OP RDE, MEYS, Czech Republic under the project CANAM OP (No. CZ.02.1.01/0.0/0.0/16_013/0001812) and by the Czech Science Foundation GACR (No. 23-06702S).

References

[1] Ermolaev G A *et al* 2020 *npj 2D Mater. Appl.* **4** 21
[2] Donnet C *et al* 1996 *Tribol. Int.* **29** 123
[3] Jiang J W, Park H S and Rabczuk T 2013 *J. Appl. Phys.* **114** 064307
[4] Kobayashi K and Yamauchi J 1995 *Phys. Rev. B* **51** 17085
[5] Li Y H *et al* 2018 *npj Comput. Mater.* **4** 49
[6] El Beqqali O *et al* 1997 *Synth. Met.* **90** 165
[7] Radisavljevic B *et al* 2011 *Nat. Nanotechnol.* **6** 147
[8] Akinwande D, Petrone N and Hone J 2014 *Nat. Commun.* **5** 5678
[9] Lopez-Sanchez O *et al* 2013 *Nat. Nanotechnol.* **8** 497
[10] Nishimura S 2001 *Handbook of Heterogeneous Catalytic Hydrogenation for Organic Synthesis* (New York: Wiley)
[11] Salazar N *et al* 2020 *Nat. Commun.* **11** 4369
[12] Tsai M L *et al* 2014 *ACS Nano* **8** 8317
[13] Yang X *et al* 2014 *J. Mater. Chem. A* **2** 7727
[14] Li X D *et al* 2013 *ACS Appl. Mater. Interfaces* **5** 8823
[15] Murugesan S *et al* 2013 *ACS Nano* **7** 8199
[16] Escalera-López D *et al* 2016 *ACS Catal.* **6** 6008
[17] Loh T A J and Chua D H C 2014 *ACS Appl. Mater. Interfaces* **6** 15966
[18] Goswami A *et al* 2017 *Nano Res.* **10** 3571
[19] Ho Y T *et al* 2015 *Phys. Status Solidi* (*RRL*) **9** 187
[20] Tumino F *et al* 2019 *Nanoscale Adv.* **1** 643
[21] Siegel G *et al* 2015 *APL Mater.* **3** 056103
[22] Borghesi M Ion acceleration: TNSA and beyond In: Gizzi L A *et al Laser-Driven Sources of High Energy Particles and Radiation* Cham: Springer 2019 doi: 10.1007/978-3-030-25850-4_7
[23] Torrisi L *et al* 1988 *Phys. Rev. B* **38** 1516
[24] Sun D *et al* 2021 *Front. Mater.* **8** 717760
[25] Khan M F *et al* 2017 *J. Mater. Chem. C* **9** 2337
[26] Sakthivel R *et al* 2021 *J. Phys.: Conf. Ser.* **2070** 012131
[27] Torrisi L *et al* 2019 *Vacuum* **160** 1
[28] Feldman L C and Mayer J W 1986 *Fundamentals of Surface and Thin Film Analysis* (New York: North-Holland)
[29] Torrisi L, Scolaro C and Restuccia N 2017 *J. Mater. Sci.: Mater. Med.* **28** 63
[30] Torrisi L, Borrielli A and Margarone D 2007 *Nucl. Instrum. Methods Phys. Res. Sec.B: Beam Interat. Mater. At* . **255** 373
[31] Dahmani F and Kerdja T 1991 *Phys. Rev. A* **44** 2649
[32] Torrisi L *et al* 2008 *Laser Part. Beams* **26** 379
[33] Torrisi L *et al* 2020 *Contrib. Plasma Phys.* **60** e201900187
[34] Torrisi L and Torrisi A 2022 *Contrib. Plasma Phys.* **62** e202200037
[35] Kandhasamy D M *et al* 2022 *ACS Omega* **7** 629
[36] Torrisi L and Torrisi A 2023 *Contrib. Plasma Phys.* **63** e202300024
[37] Tuller W N 1954 *The Sulphur Data Book* (New York: McGraw-Hill)
[38] Strazzulla G *et al* 1987 *Icarus* **70** 379
[39] NIST atomic spectra database ionization energies form. https://physics.nist.gov/PhysRefData/ASD/ionEnergy.html
[40] Gurlui S and Focsa C 2011 *IEEE Trans. Plasma Sci.* **39** 2820
[41] Láska L *et al* 2004 *Rev. Sci. Instrum.* **75** 1575
[42] Shirkov G D and Zschornack G 1996 *Electron Impact Ion Sources for Charged Heavy Ions* (Wiesbaden: Vieweg) https://www.las.ac.cn/front/ebook/detail?id=e2c99352d6ff421b053b6800f9c73d86
[43] Donnelly G E *et al* 2020 *Nanotechnology* **31** 145706
[44] Li H *et al* 2018 *J. Lumin.* **199** 210
[45] Berni M *et al* 2020 *Thin Solid Films* **709** 138258
[46] Barvat A *et al* 2018 *Mater. Today: Proc.* **5** 2241
[47] Bertoldo F *et al* 2021 *ACS Nano* **15** 2858
[48] Torrisi L *et al* 2022 *Phys. Solid State* (*A*) **219** 2100628
[49] Jiang A H *et al* 2021 *Results Phys.* **25** 104278
[50] Liu Y C and Gu F X 2021 *Nanoscale Adv.* **3** 2117